Kyle Lam is a physics major at the University of Memphis, graduating in the Spring of 2023. He hopes to attend graduate school in the Fall of 2023. Kyle has conducted research in chemistry, biology, and physics. At the University of Memphis in the summer of 2022, he participated in an NSF-funded research experience. Kyle is very thankful for the opportunity, where he learned many, new techniques in the field and made connections that he hopes to maintain in the coming years.

N.K. Lam

Synthesis of transition metal sulfides via low-pressure chemical vapor deposition

Faculty Sponsor

Dr. Shawn Pollard

Abstract

Transition metal sulfides are in a unique position to replace the roles of many existing materials currently used in renewable energy technologies. They can be more conductive and have better electrocatalytic activity than their oxide counterparts while also being cheaper and safer to use and synthesize than their telluride and selenide counterparts. However, traditional synthesis routes of transition metal sulfides are inefficient, taking several hours to produce products that are too thick to be used. Low-pressure chemical vapor deposition can avoid many of the issues of wet chemical methods. However, the morphology of transition metal sulfides synthesized using LPCVD is not well understood. Here, an evaluation of the synthesis of nickel, copper, and their molybdenum sulfides using low-pressure chemical vapor deposition is presented. The resulting growth was then characterized using SEM, EDX, and XRD. Temperature and precursor concentration have clear effects on the morphology and the density of sulfide growth.

INTRODUCTION

As the world's energy demands and consumption increase, so too does its need for more efficient and inexpensive energy storage and conversion materials. Sustainable energy is a large and still growing field of interest. Current projects include improved efficiency of current power sources like capacitors or lithium-ion batteries along with improved fuel generation methods like hydrogen evolution reaction (HER) and oxygen evolution reactions (OER).[1-3]

A growing body of research has been focused on two-dimensional (2D) nanomaterials for efficient energy storage and conversion. 2D materials also have the added benefits of high specific surface area, many sites for electrochemistry, and high mechanical flexibility.[4] Unlike their 0D, 1D, and bulk counterparts, 2D materials also have the flexibility to be synthesized using either a top-down or bottom-up approach.[5]

2D transition metal chalcogenides (TMCs) and hybrid metal chalcogenides are promising materials. 2D-TMCs have been studied for their photovoltaic, thermoelectric, semiconducting, superconducting, nanosensing, and electrocatalytic applications.[6,7] 2D-TMCs have also demonstrated potential in 2D spintronic devices, which open up avenues of research in not only renewable energy but also in quantum computing and new physical phenomena.[8,9] 2D-TMCs are able to preserve electron spin for more than 3 ns at 5 K under certain conditions, and their valley polarizations can be controlled to some extent.[10-12] In particular, nickel, copper, and molybdenum sulfides have been studied extensively.

For HER and OER, the standard electrode material is RuO2 and IrO2 due to their high electrical conductivities and low overpotentials. However, these materials are expensive and corrode easily, which produces toxic, metal ions. Nickel and copper sulfides have shown promise as possible replacements. Nickel and copper are abundant, relatively safe to work with, and cheap. They also exhibit low overpotentials, and one method to increase their conductivity is to use foams.[1,2,7,13-16] Nickel and copper foams have the benefit of being highly conductive and increasing surface area, which leads to more efficient electrodes and electrocatalysts.

However, current research on transition metal sulfide synthesis is lacking. Conventionally, nickel and copper sulfides are synthesized using hydrothermal methods. However, these processes can take several hours or even days to produce the sulfides. The sulfides also potentially suffer from nonuniformity and uneven thickness, or the process cannot reasonably be scaled up or down. An alternative synthesis pathway is through chemical

vapor deposition (CVD). Products produced through CVD can be made much more quickly than through solvothermal processes, and because of the tight control over the entire process, the sulfide can be finely tuned. Gas flow rate, temperature, the distance between precursors, the concentration of precursors, etc. can all affect the product made and the morphology of the product.

Nickel and copper sulfides can be produced on nickel and copper foams, respectively, using CVD.[2,17] However, there is little to no data on how low-pressure CVD (LPCVD) or plasma-enhanced CVD (PECVD) affects the growth and morphology of nickel and copper sulfides. There is also little on how the accessibility of growth sites, such as those on 3D foam, influences the polymorphs of the transition metal sulfides or their morphologies. While the surface growth may be of a singular phase, the phases of the foam areas that are harder to access or even the layers immediately below the surface growth are not well-characterized.

Furthermore, binary metal sulfides suffer from a similar deficit of knowledge. Although it is known that polymetallic compounds can have higher electrical conductivity and that they could be instrumental in the performance increase of supercapacitors or the creation of battery-supercapacitor hybrid devices, no study has been done on the synthesis of nickel or copper and molybdenum sulfides via LPCVD.[18-20]

As previously described, CVD has a breadth of control points, such as distance between the substrates or flow rate. Because this area has not been well explored, however, the driving variables here are primarily temperature and precursor concentration on sulfide growth. Here, an evaluation of the synthesis of nickel, copper, and their molybdenum sulfides using low-pressure chemical vapor deposition is presented.

MATERIALS AND METHODS

Synthesis

Nickel Sulfide

Sulfur powder (Alfa Aesar, 99.5% purity) and nickel foam (MTI Corporation) were used to synthesize nickel sulfides.The nickel foam was prepared into roughly 3 cm2 rectangles and precleaned using isopropanol and DI water under sonication for five minutes each.

The appropriate amounts of sulfur and the closest edge of the prepared nickel foam were placed in crucibles in a quartz tube about 13 cm apart in the furnace (MTI Corporation OTF-1200X-80-II-4CV-PE-SL). The furnace

was programmed to heat up to 150°C in 15 minutes, stay at that temperature for an additional 10 minutes, heat up to the target temperature at a rate of 10°C per minute, stay at the target temperature of either 300°C or 400°C for 15 minutes, and then stop. Figure 1 shows the heating programming. The quartz tube was placed under a vacuum, and then argon with a flow rate of 50 sccm was introduced.

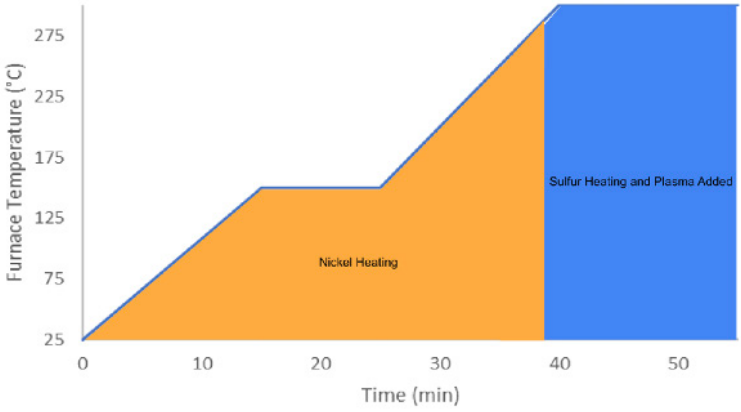

Figure 1. Heating profile of temperature program for furnace. This program is for PECVD and a target temperature of 300°C. The furnace starts at SATP. After staying at the target temperature for 15 minutes, the furnace turns off, and the product cools naturally.

The nickel was preheated to 150°C for 15 minutes by the furnace with the sulfur just outside of the furnace's range. About 20°C before the furnace reached the target temperature, the sulfur was also placed within the furnace's range, and plasma was added. The plasma was generated at 100 W and introduced 45 cm from the sulfur powder. Figure 2 shows a schematic of the CVD setup.

After the furnace reached the target temperature and both substrates were heated for about 15 minutes, the product cooled naturally, still under vacuum and with an argon flow rate of 20 sccm.

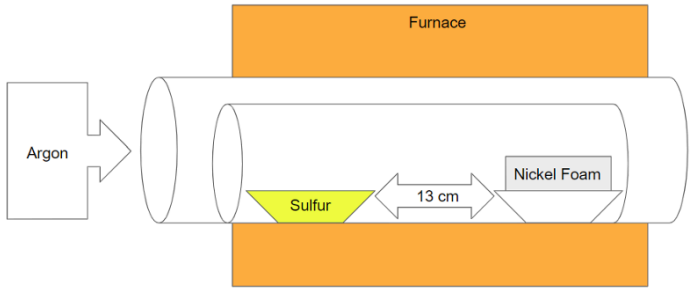

Figure 2. Schematic of PECVD setup. About 20°C before reaching the target temperature, the furnace was moved to encompass both sulfur and nickel, and plasma was added, if necessary.

Copper Sulfide

The synthesis of copper sulfide followed the same procedure as the nickel sulfide synthesis. However, the copper foam (MTI Corporation) was cut into 3.6 cm2 rectangles to prevent the foam from falling inside the crucible during loading. Plasma was also never introduced during the synthesis of copper sulfide.

Nickel-Molybdenum-Sulfur Complex

The preparation of the nickel foam and sulfur followed the same procedure as the nickel sulfide synthesis. 25 mg of molybdenum (VI) oxide (Sigma-Aldrich, ≥ 99.5% purity) was placed between the sulfur and nickel foam. It was 18 cm from the sulfur and 25 cm from the nickel foam. Figure 3 shows the setup.

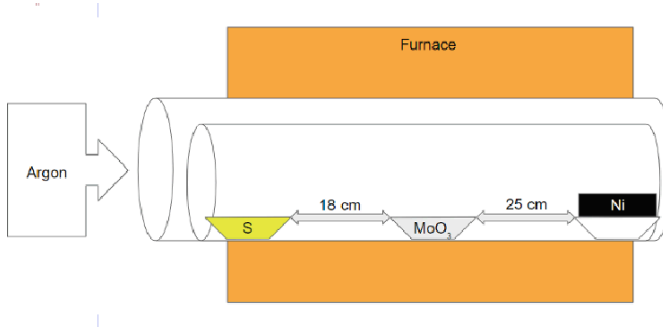

Figure 3. Schematic of LPCVD setup for synthesis of nickel-molybdenum-sulfur complex after reaching target temperature.

After placing the reactants under vacuum and then introducing argon at 50 sccm, the furnace was programmed to heat up to 300°C in 15 minutes, stay at that temperature of either 750°C or 850°C for 10 minutes, increase to the target temperature at 10°C per minute, stay at the target temperature for 15 minutes, and then stop. Figure 4 shows the heating program.

The sulfur was kept just outside of the furnace. At about 20°C before reaching the target temperature, the furnace was moved to encompass all substrates. Because of the distance between the substrates, the furnace was moved, so the sulfur was on the thermoblock and not directly in the heating zone.

Copper-Molybdenum-Sulfur Complex

The synthesis of the copper-molybdenum-sulfur complex followed mostly the same procedure as the nickel-molybdenum-sulfur complex. However, instead of placing the molybdenum (VI) oxide in a crucible between the sulfur and copper, it was placed directly underneath the copper foam. The copper foam was placed to cover about half of the MoO3's area. The sulfur and the copper foam were set 18 cm apart.

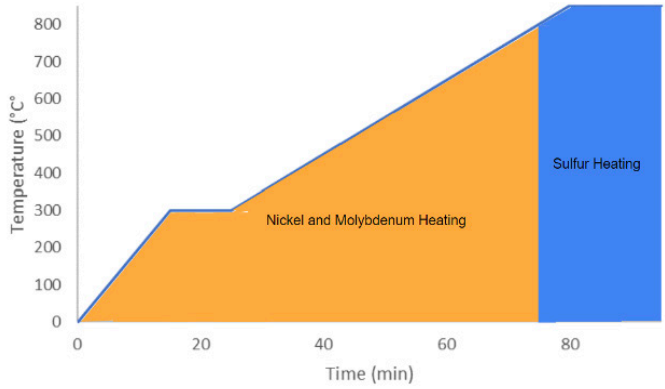

Figure 4. Heating profile of furnace programming. About 20°C before reaching the target temperature, the furnace was moved to encompass all substrates.

Characterization

X-ray diffraction (XRD) was carried out using a Bruker D8 Discover XRD to identify and characterize the crystalline structure of the sulfides and complexes on the transition metal foams. The XRD scanned the samples at 0.48 degrees per second from 10° to 80° at 20 kV.

Scanning electron microscopy (SEM) and energy dispersive x-ray spectroscopy (EDX) were carried out using a Hitachi S-4700 to identify the morphologies and elemental composition on the foam surface.

RESULTS

Figure 5 shows plain nickel and copper foams for reference.

Sulfides

Nickel Sulfide

At low concentrations of sulfur and in the presence of plasma, the sulfide growth is more uniform in texture with fewer or less pronounced peaks or branches visible in Figure 6b and Figure 6c.

The thickness of the sulfide growth is greater in the presence of plasma as shown by the crosssection in Figure 7b. At high concentrations of sulfur, however, the differences are not noticeable. The growth is evenly spread and shaped with and without plasma as seen in Figure. 8. The thickness of the growth also is equivalent.

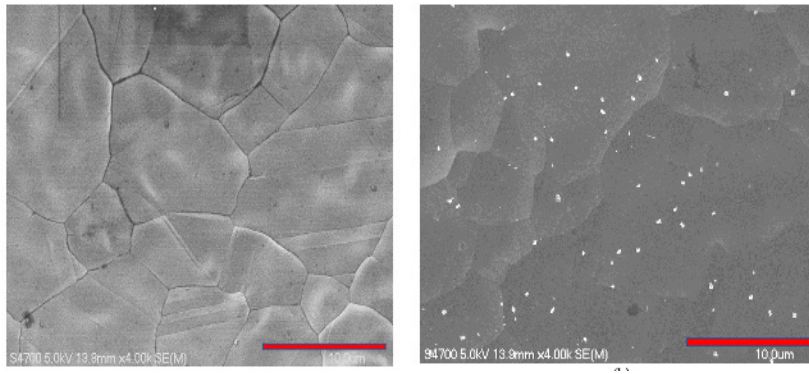

(a) (b)

Figure 5. (a) Unaltered nickel foam. (b) Unaltered copper foam.

All XRD spectra are normalized with respect to the largest nickel peak around 45°. Figures 9 and 10 show many overlapping peaks, so it is very difficult to characterize the peaks as coming from a single species.

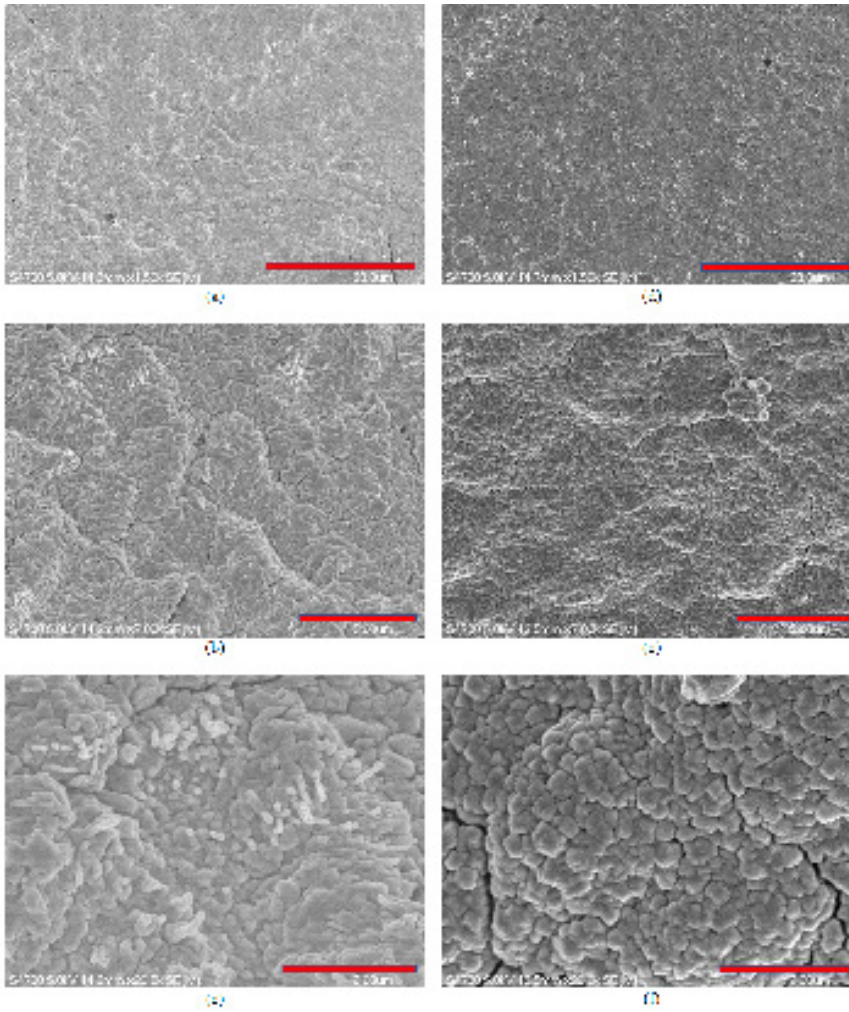

Figure 6. SEM images of nickel sulfide deposited on nickel foam with 1 mg S (a-c) without plasma and (d-f) with plasma.

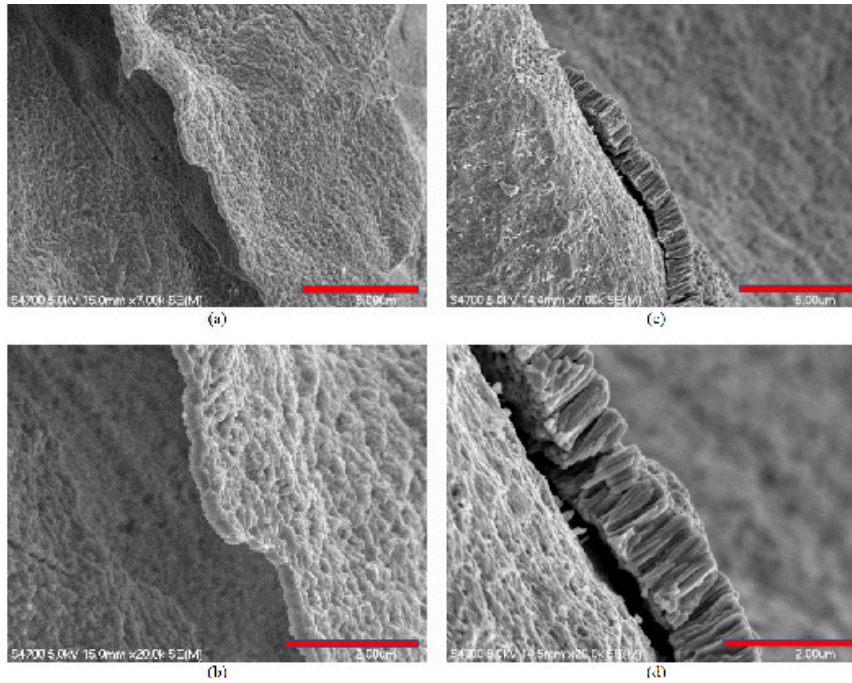

Figure 7. SEM images of nickel sulfide deposited on nickel foam with 5 mg S (a,b) without plasma and (d,e) with plasma.

Copper sulfide

Figure 11 shows sulfide deposited on copper foam. Copper sulfide grown at higher temperatures has more even growth with fewer small grains being seen at high temperatures.

The thickness of the growth also changes substantially as shown in Figure. 12. Not only is the growth thicker at higher temperatures, but the cross-section is smoother than the column-like cross-section of the lower temperature growth. Small grains can be seen on the surface of the smooth cross-section. Increasing the initial concentration of sulfur shows similar results as increasing the temperature. The growth is more even with fewer, large grains interspersed, which is consistent with previous work.

Looking beyond the surface and at lower levels of the copper foam, the growth at each layer is different, as shown in Figure 13. At lower levels, the copper foam beneath is more easily seen, and the sulfide grains are farther apart and smaller. All spectra are normalized with respect to the largest

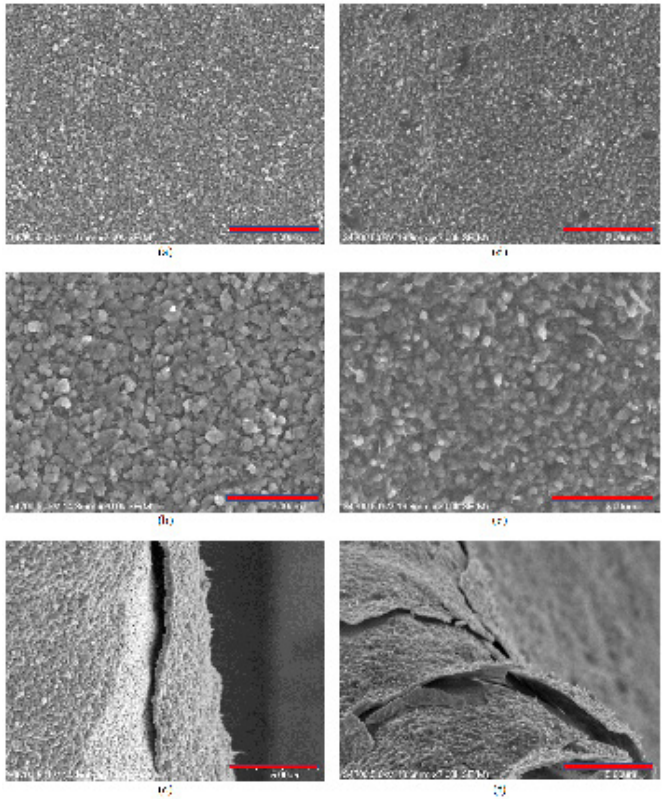

Figure 8. SEM images of nickel sulfide deposited on nickel foam with 100 mg S (a-c) without plasma and (d-f) with plasma.

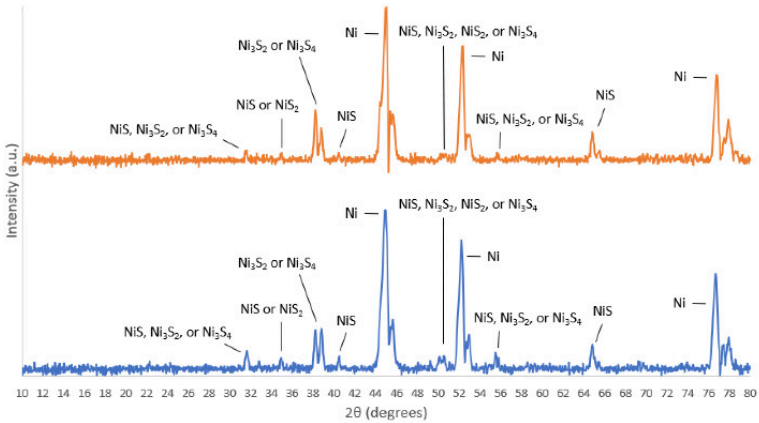

Figure 9. XRD spectrum of nickel sulfide on nickel foam with 1 mg S. Blue is without plasma; orange is with plasma.

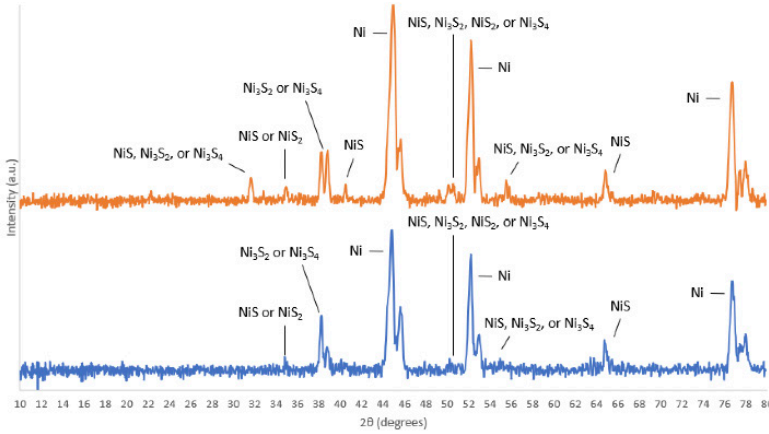

Figure 10. XRD spectrum of nickel sulfide on nickel foam. Blue is the sample grown with 1 mg S; orange is the sample grown with 100 mg S.

copper peak around 44 degrees. The spectra in Figures 14 and 15 show that the initial concentration of sulfur does affect the species of copper sulfide synthesized. Like with nickel sulfide, there is much overlap between the samples, which makes it difficult to characterize the peaks as coming from a single species.

Transition Metal-Molybdenum-Sulfur Complex

Nickel-Molybdenum-Sulfur

The SEM images in Figure 16 show that the nickel-molybdenum-sulfur complexes grown at different temperatures have clear, morphological differences. The samples grown at 750°C had more globular growth while the samples grown at 850°C had nonuniform growths.

For the growth at lower temperatures, the XRD spectra in Figure 17 suggest the presence of many different crystalline structures within the sample. For the growth at higher temperatures, however, the XRD spectrum has significantly fewer peaks.

Copper-Molybdenum-Sulfur

The samples grown at lower concentrations of sulfur in Figure 18 show larger, more uniformly shaped grains while the samples grown at high concentrations of sulfur are less uniform in shape. The growths appear to be melted together.The morphologies at different temperatures also differ.

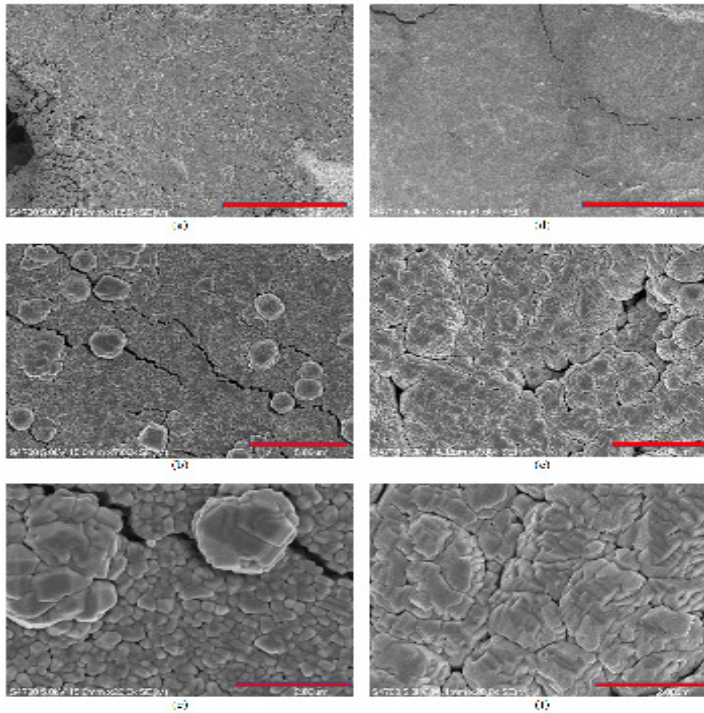

Figure 11. SEM images of copper sulfide deposited on copper foam with 1 mg S at (a-c) 300°C and (d,e) 500°C.

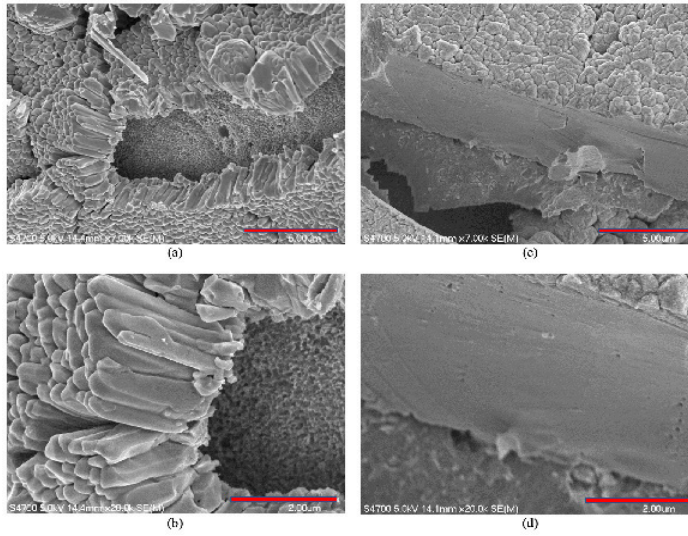

Figure 12. SEM images of copper sulfide deposited on copper foam with 5 mg S at (a-c) 300°C and (d,e) 500°C.

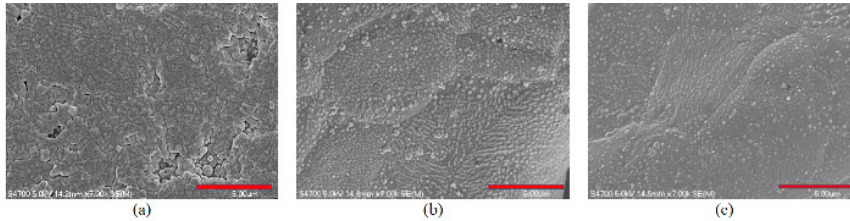

Figure 13. SEM images of copper sulfide deposited on copper foam with 5 mg S (a) one layer below the surface (b) two layers below the surface (c) three layers below the surface.

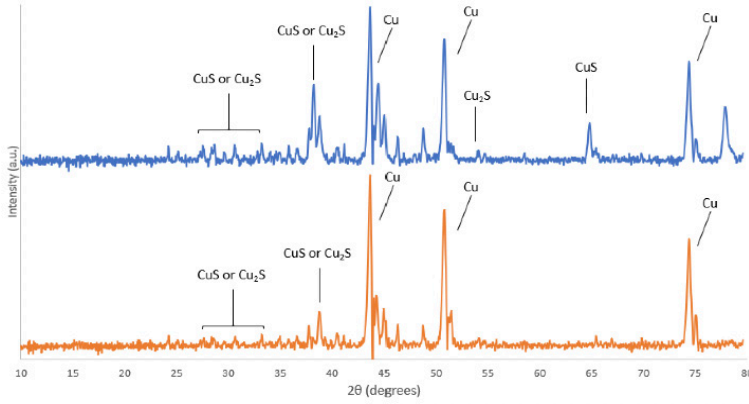

Figure 14. XRD spectra of copper sulfide on copper foam at 300°C. Blue is the sample grown with 1 mg S; orange is the sample grown with 5 mg S.

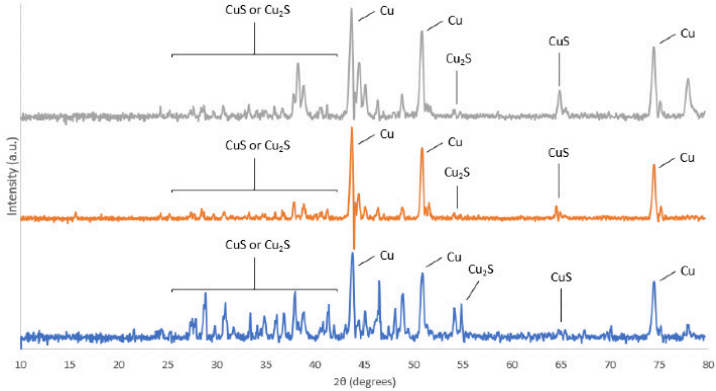

Figure 15. XRD spectra of copper sulfide on copper foam. Samples were grown with 5 mg S at (gray) 300°C, (orange) 500°C, and (blue) 750°C.

The sample grown at a higher temperature has sharper, more well-defined structures than the sample grown at a lower temperature as shown in Figure 19.

Looking beyond the surface and at lower levels of the copper foam in Figure 20, the growth at each layer is different. At lower levels, the copper foam beneath is more easily seen, and irregularly-shaped growths start to appear.All spectra in Figures 21 and 22 were normalized with respect to peaks around 38 degrees. Like with the nickel-molybdenum-sulfur complex, the spectra suggest the presence of many different crystalline structures.

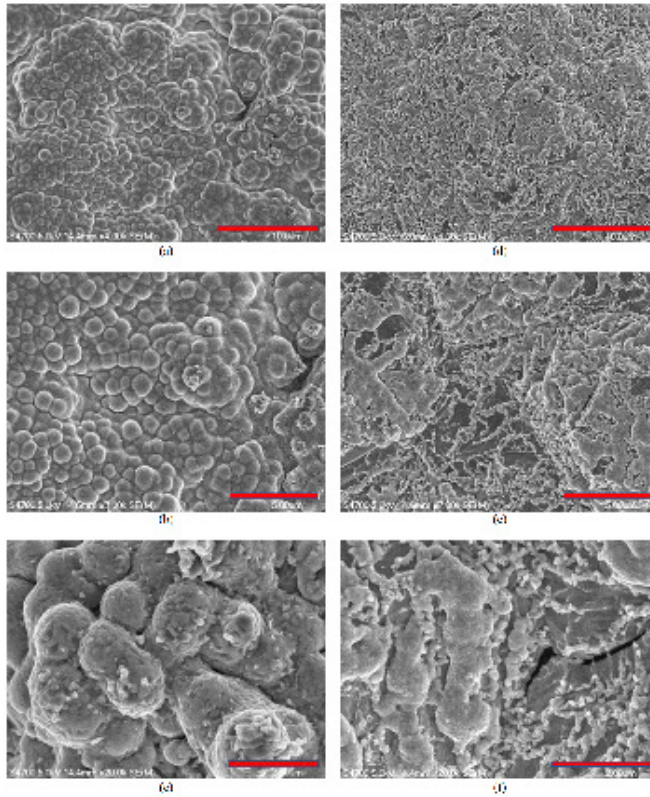

Figure 16. SEM images of nickel-molybdenum-sulfur complexes. The samples were grown with 500 mg S and 25 mg MoO3 at (a-c) 750°C and (d-f) 850°C.

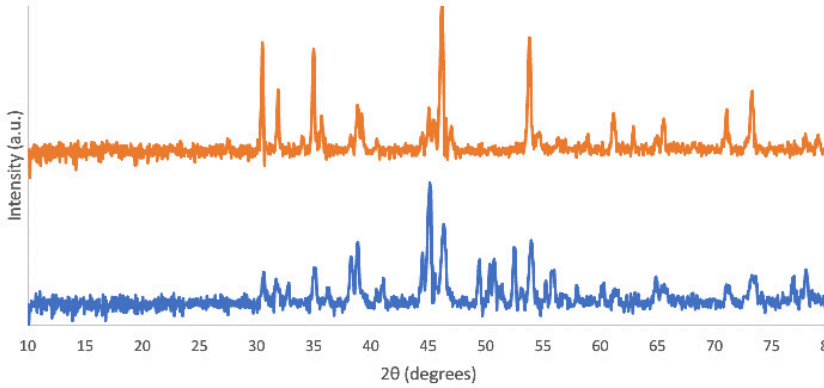

Figure 17. XRD spectra of nickel-molybdenum-sulfur samples grown with 500 mg S and 25 mg MoO3. Blue is the sample grown at 750°C; orange is the sample grown at 850°C.

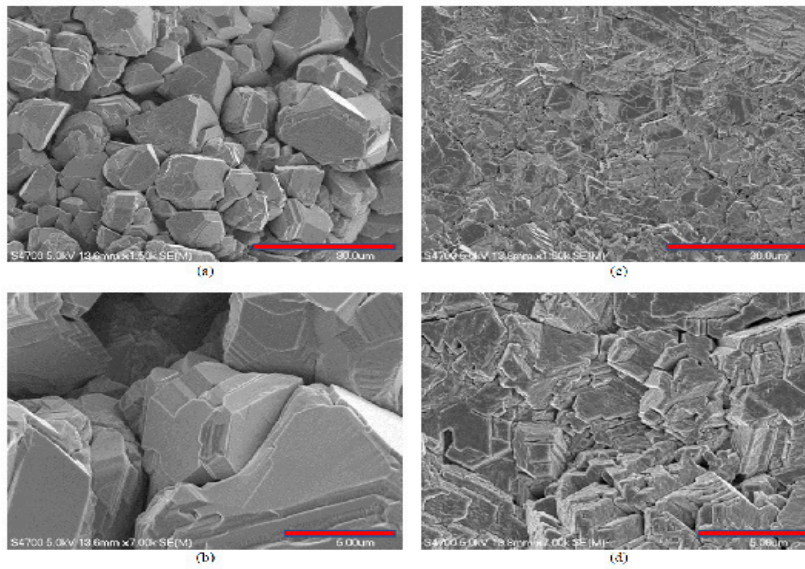

Figure 18. SEM images of copper-molybdenum-sulfur complexes. All samples were grown with 10 mg MoO3 at 750°C using (a,b) 50 mg S and (c,d) 500 mg S.

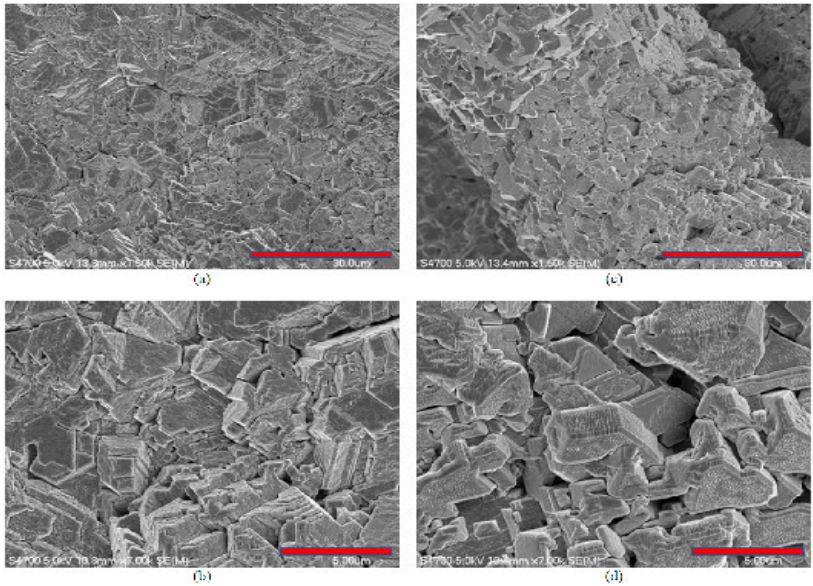

Figure 19. SEM images of copper-molybdenum-sulfur complexes. The samples were grown using 500 mg S and 10 mg MoO3 at (a,b) 750°C and at (c,d) 850°C.

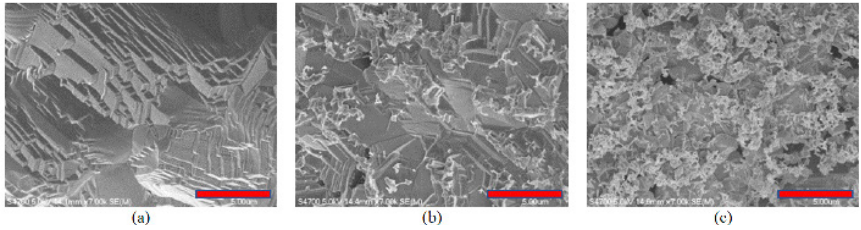

Figure 20. SEM images of the copper-molybdenum-sulfur complex growth (a) one layer below the surface (b) two layers below the surface (c) three layers below the surface.

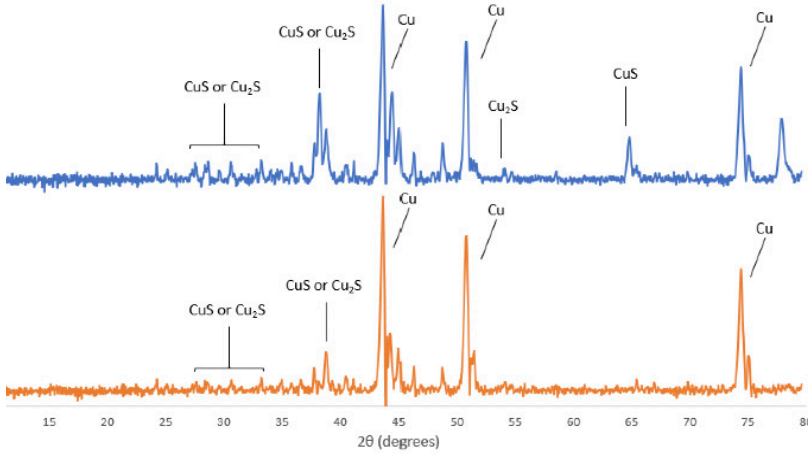

Figure 21. XRD spectra of copper-molybdenum-sulfur samples grown with 500 mg S and 10 mg MoO3. Orange is the samples grown at 750°C; blue is the sample grown at 850°C.

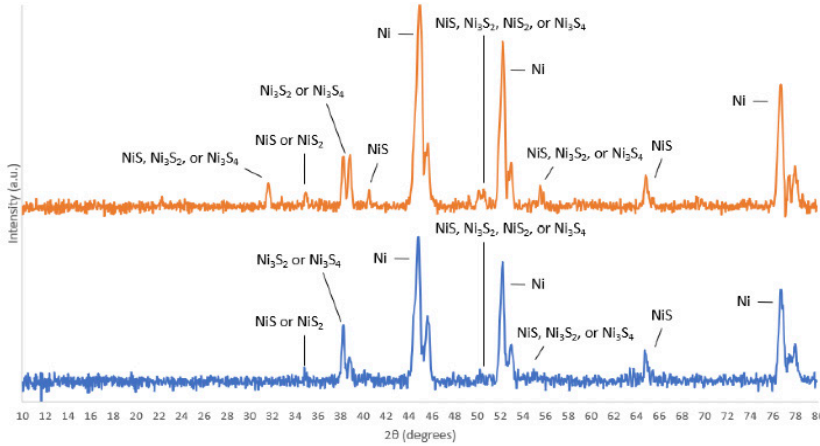

Figure 22. XRD spectra of copper-molybdenum-sulfur samples grown at 850°C with 10 mg MoO3. Orange is the sample grown with 50 mg S; blue is the sample grown with 500 mg S.

DISCUSSION

Transition Metal Sulfides

Nickel Sulfide

The presence of plasma affects the surface morphology of the nickel sulfides with the plasma making the growth more uniform in size and density up to about 5 mg of sulfur. At high concentrations of sulfur, such as in the 100 mg samples, the surface morphologies and thickness were about the same.

Sulfur concentration and plasma do not affect the crystallinity of nickel sulfides produced as shown by the XRD spectra. Based on the XRD spectra, it seems that the temperature has a greater effect on the crystallinity than the concentration, but both affect the morphology. The XRD fitting software suggests that there is a mix of species of roughly the same stoichiometric coefficients, such as NiS1.3 and NiS1.17. The non-uniformity of the foam's geometry may have also influenced the XRD spectra.

Copper Sulfides

Temperature and sulfur concentration have noticeable effects on the growth of copper sulfide with increasing temperatures and concentrations producing larger and more uniform grains.The accessibility of nucleation sites also affects growth. The less accessible fourth layer of copper foam has higher copper content, and what little sulfide has grown on the surface is much smaller in size and density than the easily accessible top layer.

Like nickel sulfide, the crystallinity of copper sulfides remains constant at low concentrations of sulfur and over a wide temperature range. The crystallinity changes significantly only at 750°C.

Transition Metal-Molybdenum-Sulfur Complexes

Nickel-Molybdenum-Sulfur

The nickel-molybdenum-sulfur complex was successfully synthesized. First, nickel oxide was synthesized more quickly than the complex, which led to the nickel foam melting. However, by placing the MoO3 in a separate crucible 25 cm away from the nickel foam, nickel oxide was not able to outpace the growth of the complexes.

Temperature has a significant effect on the morphology and crystal structure of the complex. At higher temperatures, the growth appears to have melted together or conglomerated into larger structures. It is possible that, like the nickel and copper sulfides, there are more phases present at 750°C than at 850°C.

Like with copper sulfide, temperature and sulfur concentration have effects on morphology and crystal structure. At higher concentrations of sulfur, the growth loses its smooth, well-defined structures and develops a rougher, denser growth pattern. However, the structure appears to become more separated and well-defined again at higher temperatures.

The accessibility of nucleation sites also affects growth with the first layer being the outermost surface and subsequent layers closer to the center of the foam. The less accessible fourth layer of copper foam has higher copper content, and unlike the higher, more accessible levels, the growth does not have relatively smooth and sharp morphology. Instead, there are randomly shaped and oriented growths.

Unlike the transition metal sulfides or the nickel-molybdenum-sulfur complex, the XRD spectra for the copper-molybdenum-sulfur complexes remained complex regardless of temperature or sulfur concentration.

Conclusion

The presence of plasma seemed to have little effect on both the morphology and the crystal structure of the resultant transition metal sulfide. Temperature and sulfur concentration had significantly more effect, but while sulfur concentration influenced only morphology, temperature impacted both structure and morphology. The results match previous work.

FUTURE WORK

In addition to further investigation on the relation between concentration and temperature on surface morphology and crystal structure, future projects will focus on the electrocatalytic activity of the transition metal sulfides and binary metal sulfides. The application of these materials in electrodes for HER or OER is promising but has not been fully explored.

In these experiments, the temperature and precursor concentrations were the driving variables in morphology and crystal structure because the relation between these factors on the growth on foam was not well understood. Other work can also include the other variables that come with CVD, such as the addition of plasma or the effect of flow rate differences.The activity of the other chalcogenides, selenium and tellurium, should also be evaluated.

References

1. X. Zheng, X. Han, Y. Zhang, J. Wang, C. Zhong, Y. Deng, and W. Hu, Nanoscale 11, 5646 (2019).

2. M. Kajbafvala, O. Moradlou, and A.Z. Moshfegh, Vacuum 188, 110209 (2021).

3. S.M. Dinara, A.K. Samantara, J.K. Das, J.N. Behera, S.K. Nayak, D.J. Late, and C.S. Rout, Dalton Trans. 48, 16873 (2019).

4. X. Peng, L. Peng, C. Wu, and Y. Xie, Chem. Soc. Rev. 43, 3303 (2014).

5. Z. Cai, B. Liu, X. Zou, and H.-M. Cheng, Chem. Rev. 118, 6091 (2018).

6. R.A. Hussain, A. Badshah, and B. Lal, Journal of Solid State Chemistry 243, 179 (2016).

7. A.P. Tiwari, Y. Yoon, T.G. Novak, K.-S. An, and S. Jeon, ACS Appl. Nano Mater. 2, 5061 (2019).

8. W. Zhang, P.K.J. Wong, R. Chua, and A.T.S. Wee, in Spintronic 2D Materials (Elsevier, 2020), pp. 227–251.

9. Q.H. Wang, K. Kalantar-Zadeh, A. Kis, J.N. Coleman, and M.S. Strano, Nature Nanotech 7, 699 (2012).

10. L. Yang, N.A. Sinitsyn, W. Chen, J. Yuan, J. Zhang, J. Lou, and S.A. Crooker, Nature Phys 11, 830 (2015).

11. H. Zeng, J. Dai, W. Yao, D. Xiao, and X. Cui, Nature Nanotech 7, 490 (2012).

12. K.F. Mak, K. He, J. Shan, and T.F. Heinz, Nature Nanotech 7, 494 (2012).

13. M.A. Ehsan, A. Rehman, A. Afzal, A. Ali, A.S. Hakeem, U.A. Akbar, and N. Iqbal, Energy Fuels 35, 16054 (2021).

14. J. Yoo, I.H. Kwak, I.S. Kwon, K. Park, D. Kim, J.H. Lee, S.A. Lim, E.H. Cha, and J. Park, J. Mater. Chem. C 8, 3240 (2020).

15. Y.-Z. Xu, C.-Z. Yuan, and X.-P. Chen, Journal of Solid State Chemistry 256, 124 (2017).

16. J. Du, Y. Qian, L. Wang, H. Yang, and D.J. Kang, Materials Today Communications 25, 101585 (2020).

17. Y. Fu, Q. Li, J. Liu, Y. Jiao, S. Hu, H. Wang, S. Xu, and B. Jiang, Journal of Colloid and Interface Science 570, 143 (2020).

18. T. Ma, J. Chen, M. Chen, S. Liu, J. Luo, H. Zou, W. Yang, and S. Chen, Journal of Alloys and Compounds 838, 155631 (2020).

19. W. Chen, P. Yuan, S. Guo, S. Gao, J. Wang, M. Li, F. Liu, J. Wang, and J.P. Cheng, Journal of Electroanalytical Chemistry 836, 134 (2019).

20. Y.-Y. Huang and L.-Y. Lin, ACS Appl. Energy Mater. 1, 2979 (2018).